

Comparative calculation on Li^+ solvation in common organic electrolyte solvents for lithium ion batteries*

Qi Liu(刘琦), Feng Wu(吴锋)[†], Daobin Mu(穆道斌)[‡], and Borong Wu(吴伯荣)

Beijing Key Laboratory of Environment Science and Engineering, School of Material Science and Engineering,
Collaborative Innovation Center of Electric Vehicles in Beijing, Beijing Institute of Technology, Beijing 100081, China

(Received 6 October 2019; revised manuscript received 8 February 2020; accepted manuscript online 13 February 2020)

It is important for the electrolytes to maintain and enhance the lithium ion battery electrochemical performance, and solvation of Li^+ is a key parameter for the property of the electrolytes. The comparative study on Li^+ solvation structures, energy, enthalpy, Gibbs free energy, infrared and Raman spectra in common organic electrolyte solvents is completed by density functional theory (DFT) method. The solvation reaction energy results suggest that the Li^+ solvation priority order is propylene carbonate (PC) > ethylene carbonate (EC) > ethyl methyl carbonate (EMC) > diethyl carbonate (DEC) > tetrahydrofuran (THF) > dimethyl carbonate (DMC) > 1,3-dioxolane (DOL) > dimethoxyethane (DME) to form 5sol- Li^+ . It is also indicated that the most innermost solvation shell compounds formations by stepwise spontaneous solvation reaction are four cyclic solvent molecules and three linear solvent molecules combining one Li^+ forming 4sol- Li^+ and 3sol- Li^+ , respectively, at room temperature. Besides, the vibration peaks for C=O and C–O bonds in carbonate ester solvents- Li^+ compounds shift to lower frequency and higher frequency, respectively, when the Li^+ concentration increases in the solvation compounds. All Li–O stretching vibration peaks shift to higher frequency until forming 2solvent- Li^+ complexes, and C–H stretching also shifts to higher frequency except for *n*DME- Li^+ solvation compounds. The Raman spectrum is more agile to characterize C–H vibrations and IR is agile to C=O, C–O, and Li–O vibrations for Li^+ solvation compounds.

Keywords: Li^+ solvation, frequency shift, infrared spectra, Raman spectra

PACS: 82.45.–h, 78.30.–j

DOI: 10.1088/1674-1056/ab75cc

1. Introduction

The development of renewable energy sources is very essential,^[1,2] owing to the continuous consumption of fossil fuels.^[3] Lithium ion battery as a high energy density electrochemical energy storage device has been widely applied in electric automobile and intelligent electronic equipment.^[4–9] In addition, other higher energy density battery, such as Li–S battery, has also been widely focused.^[10–14] Electrolytes are key components for the electrochemical energy storage,^[15,16] and organic carbonate esters and ethers based solvents are commonly used in lithium ion battery^[17–20] and Li metal battery,^[21–24] respectively. The research on the physical chemical property of the electrolyte is important for guiding and enhancing the lithium ion battery electrochemical performance, and solvation is the key parameter of the property of the electrolytes.

Matsuda *et al.* have studied lithium ion solvation through electrospray ionization mass spectroscopy in mixed organic electrolytes. Their results have indicated that Li^+ is mainly solvated by two organic solvent molecules, and the inclination for solvation to Li^+ order is propylene carbonate (PC)

> ethylene carbonate (EC) = gamma-butyrolactone (GBL) > diethyl carbonate (DEC) > dimethyl carbonate (DMC).^[25] Molecular dynamics simulations have indicated that Li^+ and LiTFSI are solvated by 3.8 EC molecules in the condition of incompletely dissociation, and with the increase of the salt concentration, one EC molecule is replaced by one TFSI[–] anion.^[26] Electrolytes Raman spectra analysis has showed that PC molecules have selective solvation, the solvation numbers for PC molecules combining lithium ion are drastically different in DMC: PC (1 : 1 vol.) and DMC: PC (7 : 1 vol.).^[27] The EC- Li^+ complexes electronic structures have also been studied by density functional theory (DFT) method.^[28] Structural analysis in the EC- Li^+ complex has exhibited that only $\text{Li}^+ \cdots \text{O}=\text{C}$ interaction type is supported by the analysis of spectral vibration between one EC molecule and Li^+ , and the 4-coordinated stable solvation shell is supported by the analysis of Mulliken charge, electron affinity, and solvation energy among $[(\text{EC})_n-\text{Li}^+]_n = 1-5$ complexes. NMR spectroscopy also has indicated EC combining with Li^+ stronger than that of DEC or DMC.^[29] Li^+ interaction with individual carbonate molecules has been con-

*Project supported by International Science & Technology Cooperation of China (Grant No. 2019YFE0100200), the National Natural Science Foundation of China (Grant No. 51902024), the National Postdoctoral Program for Innovative Talents of China (Grant No. BX20180038), China Postdoctoral Science Foundation (Grant No. 2019M650014), NASF, China (Grant No. U1930113), and Beijing Natural Science Foundation, China (Grant No. L182022).

[†]Corresponding author. E-mail: wufeng863@vip.sina.com

[‡]Corresponding author. E-mail: mudb@bit.edu.cn

ducted by natural abundance ^{17}O -NMR measurements. The largest changes occurred in ^{17}O chemical shift at the carbonyl oxygen of EC, indicating that Li^+ prefers EC compared with DMC, and Li^+ is mainly coordinated to carbonyl-oxygens rather than ethereal-.^[30] Theoretical analysis on de-solvation has indicated that Li^+ shows bigger de-solvation energies compared to Na^+ because of the stronger Lewis acidity, and the solvation structures of Na^+/Li^+ -complexes are close to each other.^[31] DFT calculations have been performed in lithium ion batteries for EC-based binary mixtures electrolyte, it is indicated that the binary EC-based electrolyte with high EC content is stable and favorable.^[32] High concentration ether based electrolyte has been proved to enhance the Li-S battery electrochemical performance.^[33] Our previous study has indicated that high concentration carbonate ester electrolyte enjoys de-solvation compared with diluted electrolyte, and the de-solvation effect reduces the charge transfer resistance at the electrolyte/cathode interface.^[34] In addition, super-concentrated carbonate ester electrolytes with LiPF_6 ^[35] or LiFSI ^[36] salts have been reported to improve the electrochemical performance for the cathode of $\text{LiNi}_{0.5}\text{Mn}_{1.5}\text{O}_4$ high-voltage material. Ong *et al.* have found that ether oxygens or carbonyl atoms contribute to Li^+ solvation in the solvents and sometimes Li^+ is solvated by PF_6^- anion through first-principles calculation, and tetrahedral coordination is formed for different solvent species of the initial Li^+ solvation shell.^[37] The solvation structures of LiPF_6 in organic carbonate electrolyte have been investigated by DFT methods and NMR and FTIR spectroscopy. In low salt concentrations (< 1.2 M), the main species is the solvent-separated ion pair, in high salt concentrations (> 2.0 M), the main species in the electrolyte is the contact ion pair.^[38] Dahn *et al.*'s study has showed that the additive methyl acetate (MA) in carbonate ester electrolyte increases the ionic conductivity significantly and decreases the viscosity on a wide salt concentration range.^[39] Electrospray-ionization mass spectra test on varied ratios of 1,3-dioxolane (DOL)/dimethoxyethane (DME) electrolytes has suggested that $[\text{Li}(\text{DME})_2]^+$ solvation species are dominant when electrolyte compositions contain DME ($> 10\%$ in vol.).^[40] Shi *et al.*'s study has indicated that multi-scale computation methods are benefited to predict the path-independent properties, as well as close some of the current technological and experimental gaps.^[41] Quantum chemistry computations have been used to study the electrolyte solvation and battery property.^[42–49] However, comparisons on the solvation of Li^+ in different solvents, number and Li^+ solvation ratio, etc. are still unclear. These are critical to design and optimize the electrolytes of lithium ion batteries.

In this work, carbonate esters of PC, EC, DMC, ethyl methyl carbonate (EMC), DEC and ethers of DOL, DME, tetrahydrofuran (THF) solvents are studied to deeply com-

pare the physical chemistry properties of electrolyte dissolution, Li^+ migration, solvation with different Li^+ concentration. The solvation structures, energy, enthalpy, Gibbs, infrared spectroscopy, and Raman spectrum are calculated. It is demonstrated that the solvation energy is changed and the vibration frequency is shifted in different Li^+ concentration for the solvent- Li^+ compounds. The detailed calculation and discussion will be reported in the next.

2. Computation details

Becke's three parameters (B3) exchange functional along with the Lee–Yang–Parr (LYP) nonlocal correlation functional (B3LYP) is used for the DFT calculation. B3LYP/6-311++G(d,p) level is completed for all the structure optimizations, the frequency calculation at equal level is conducted to analyze the theoretical spectra. The higher level of B3LYP/6-311++G(3df,3dp) is performed to calculate ΔE at absolute zero for all single point energy to improve the calculation accuracy. The calculation of energy is also revised by the zero-point energy. Enthalpies and Gibbs free energies are computed at 25 °C, ΔH (Δ thermal correction of enthalpy by frequency analysis $+\Delta E$ (B3LYP/6-311++G(3df,3dp))) and ΔG (Δ thermal correction of Gibbs free energy by frequency analysis $+\Delta E$ (B3LYP/6-311++G(3df,3dp))). All quantum chemistry computations are performed by employing the Gaussian 09 program package.^[50]

3. Results and discussion

As we all know, the mixture of cyclic and linear carbonate esters is excellent co-solvent or mix-solvent for lithium ion battery electrolytes, and ether solvents are well matched with the higher energy density of the Li-S battery. The solvation of common organic electrolyte solvents for lithium ion battery and lithium metal battery with different Li^+ concentration is calculated by DFT method.

3.1. Carbonate ester solvation with Li^+

3.1.1. Solvation and infrared spectrum for PC, EC, and DMC with Li^+

Figure 1(a) exhibits the ΔG plots for Li^+ solvation reactions with EC, PC, and DMC respectively. The stepwise solvation reactions are helpful to identify the thermodynamic equilibrium of the solvation reactions. It can be seen that four solvent molecules spontaneously combine one Li^+ forming the solvation compound of 4sol-Li^+ at most for cyclic EC and PC solvents by the stepwise solvation reaction according to the free energy ΔG for thermodynamics equilibrium. The ΔE , ΔH , and ΔG (in kcal/mol) for the solvation reactions between Li^+ and EC, PC, DMC are also shown in

Table 1. It is non-spontaneous for $4\text{EC-Li}^+ + \text{EC} = 5\text{EC-Li}^+$ and $4\text{PC-Li}^+ + \text{PC} = 5\text{PC-Li}^+$ reactions at room temperature. However, three linear DMC solvent molecules can spontaneously combine one Li^+ at most forming 3DMC-Li^+ compounds at room temperature. The reaction of $3\text{DMC-Li}^+ + \text{DMC} = 4\text{DMC-Li}^+$ is non-spontaneous. The total

solvation reaction energies for $5\text{EC} + \text{Li}^+ = 5\text{EC-Li}^+$, $5\text{PC} + \text{Li}^+ = 5\text{PC-Li}^+$, and $5\text{DMC} + \text{Li}^+ = 5\text{DMC-Li}^+$ can be obtained as -130.286 kcal/mol, -132.2 kcal/mol, and -110.212 kcal/mol, respectively. Therefore, the DFT calculation indicates that cyclic EC and PC is prior to solvation compared with linear DMC molecule.

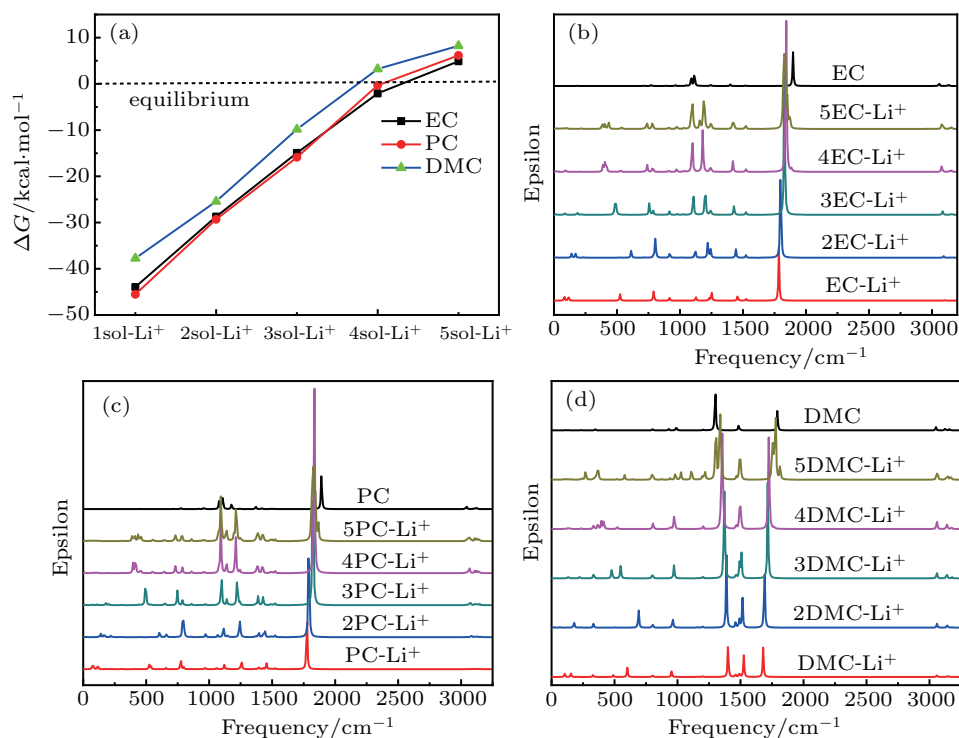


Fig. 1. (a) The ΔG plots for Li^+ solvation reactions with EC, PC, and DMC respectively. Theoretical infrared spectra of (b) EC, (c) PC, and (d) DMC solvation Li^+ complexes with different solvent numbers.

Table 1. The ΔE , ΔH , and ΔG (in kcal/mol) for the solvation reactions between Li^+ and EC, PC, DMC respectively.

Reactions in Li^+ and solvents	ΔE	ΔH	ΔG
$\text{EC} + \text{Li}^+ = \text{EC-Li}^+$	-50.296	-50.732	-43.933
$\text{EC} + \text{EC-Li}^+ = 2\text{EC-Li}^+$	-37.396	-36.811	-28.710
$\text{EC} + 2\text{EC-Li}^+ = 3\text{EC-Li}^+$	-22.307	-21.571	-14.928
$\text{EC} + 3\text{EC-Li}^+ = 4\text{EC-Li}^+$	-12.894	-12.276	-2.072
$\text{EC} + 4\text{EC-Li}^+ = 5\text{EC-Li}^+$	-7.393	-6.828	4.883
$\text{PC} + \text{Li}^+ = \text{PC-Li}^+$	-51.930	-52.380	-45.521
$\text{PC} + \text{PC-Li}^+ = 2\text{PC-Li}^+$	-38.178	-37.581	-29.305
$\text{PC} + 2\text{PC-Li}^+ = 3\text{PC-Li}^+$	-22.341	-21.591	-15.891
$\text{PC} + 3\text{PC-Li}^+ = 4\text{PC-Li}^+$	-12.756	-12.185	-0.313
$\text{PC} + 4\text{PC-Li}^+ = 5\text{PC-Li}^+$	-6.995	-6.398	6.151
$\text{DMC} + \text{Li}^+ = \text{DMC-Li}^+$	-44.384	-44.886	-37.731
$\text{DMC} + \text{DMC-Li}^+ = 2\text{DMC-Li}^+$	-33.571	-32.993	-25.422
$\text{DMC} + 2\text{DMC-Li}^+ = 3\text{DMC-Li}^+$	-19.255	-18.537	-9.833
$\text{DMC} + 3\text{DMC-Li}^+ = 4\text{DMC-Li}^+$	-8.272	-7.665	3.223
$\text{DMC} + 4\text{DMC-Li}^+ = 5\text{DMC-Li}^+$	-4.730	-4.296	8.221

Theoretical infrared spectrum of EC solvation Li^+ compounds with different solvent numbers is shown in Fig. 1(b). The C=O double bonds stretching vibration peaks are assigned on the frequency of $1784\text{--}1897$ cm^{-1} for $n\text{EC-Li}^+$ compounds. It is clearly shown that the C=O peak shifts to higher frequency when the lithium ion concentration goes

down, demonstrating that the C=O double bond is relatively shortened. The results are in agreement with the experiment infrared spectra that the C=O absorption frequency is shifted to lower wavenumber in higher salt concentration carbonate ester electrolyte.^[34] The C–O bond stretching vibration is assigned to the two peaks in $1089\text{--}1251$ cm^{-1} for $n\text{EC-Li}^+$. It is shown that the peaks of C–O group shift to lower frequency with EC molecule increase, indicating that the C–O peaks of EC shift to higher frequency direction in high salt concentration electrolyte. The two stretching vibration peaks in $390\text{--}805$ cm^{-1} represent O–Li bond in $n\text{EC-Li}^+$ solvation compounds. The O–Li vibration peaks shift to higher frequency when the lithium ion concentration increases until 2EC-Li^+ , and there are no O–Li vibration peaks observed in single EC molecule. Figure 1(c) shows the theoretical infrared spectrum of PC solvation Li^+ complexes with different solvent numbers. The peak in $1775\text{--}1892$ cm^{-1} and the two peaks in $1077\text{--}1257$ cm^{-1} are ascribed to C=O and C–O bond stretching vibrations, respectively. The Li–O bond stretching vibration is assigned to the two peaks in $390\text{--}798.5$ cm^{-1} . The frequency shift rule in PC is in agreement with that of EC. Figure 1(d) shows the theoretical infrared spectrum of DMC

solvation Li^+ complexes with different Li^+ concentration. It is shown that the vibration peak in $1679\text{--}1792.7\text{ cm}^{-1}$ represents C=O stretching. The two vibration peaks in $1299\text{--}1526\text{ cm}^{-1}$ are ascribed to the carbonate O–C stretching. The peaks in $270.62\text{--}690.7\text{ cm}^{-1}$ are the Li–O stretching vibration. The peaks shift rule for C=O, carbonate O–C, and Li–O bonds is similar to EC and PC. But the methyl C–O bond in $953.4\text{--}990.4\text{ cm}^{-1}$ slightly shifts to higher frequency with the DMC molecule increase in the solvation structure.

3.1.2. Theoretical Raman spectrum for Li^+ solvation in PC, EC, and DMC

The solvation structure models of $n\text{EC-Li}^+$, $n\text{PC-Li}^+$, and $n\text{DMC-Li}^+$ are also shown in Fig. 2(a). According to previous experimental and theoretical studies, the solvation interaction between Li^+ and solvents is the O–Li interaction, and for carbonate esters solvent, Li^+ is mainly coordinated to carbonyl-oxygens (C=O) rather than ethereal– (C–O).^[23,29,30]

On the basis of the most likely initial configuration of the Li^+ solvation structure by $\text{C}=\text{O}\cdots\text{Li}^+$ interaction in carbonate solvents, the solvation structures are optimized by DFT calculation to obtain the low energy state structure. It can be seen that Li^+ is combined and surrounded by the C=O bond of solvent molecules, and the solvation structures are in agreement with the Gibbs free energy change. Table 2 shows the O–Li bond and average length in $n\text{EC-Li}^+$, $n\text{PC-Li}^+$, and $n\text{DMC-Li}^+$. The average O–Li bond lengths in EC-Li^+ , 2EC-Li^+ , 3EC-Li^+ , 4EC-Li^+ , and 5EC-Li^+ are 1.739 \AA , 1.791 \AA , 1.857 \AA , 1.941 \AA , and 2.577 \AA , respectively. The average O–Li bond lengths in PC-Li^+ , 2PC-Li^+ , 3PC-Li^+ , 4PC-Li^+ , and 5PC-Li^+ are 1.735 \AA , 1.788 \AA , 1.856 \AA , 1.944 \AA , and 2.519 \AA , respectively. The average O–Li bond lengths in DMC-Li^+ , 2DMC-Li^+ , 3DMC-Li^+ , 4DMC-Li^+ , and 5DMC-Li^+ are 1.735 \AA , 1.785 \AA , 1.856 \AA , 1.957 \AA , and 2.090 \AA , respectively.

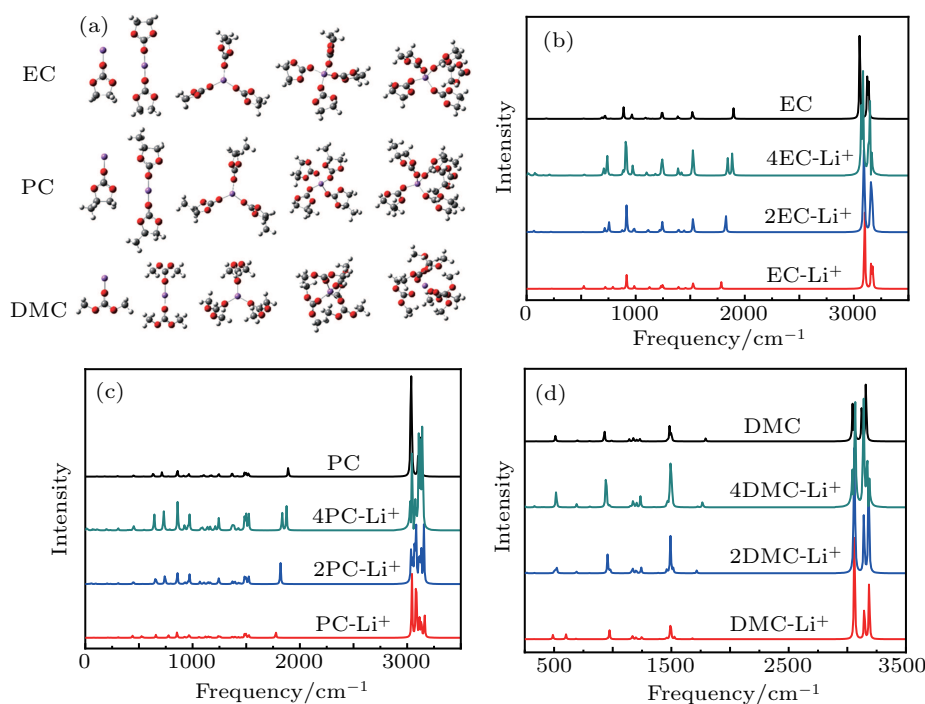


Fig. 2. (a) The solvation structure models of $n\text{EC-Li}^+$, $n\text{PC-Li}^+$, and $n\text{DMC-Li}^+$. White, dark gray, violet, and red spheres represent H, C, Li, and O ions/atoms, respectively. Theoretical Raman spectra of (b) EC, (c) PC, and (d) DMC solvation Li^+ complexes with different Li^+ concentration.

It is indicated that the O–Li bond is shortened when the solvent number decreases in the Li^+ -solvation compounds, and the Li^+ solvation ionic radius is decreased when the lithium ion concentration increases. The decrease of the Li^+ solvation ionic radius may enhance the mobility in the electrolyte. Previous experiment and theoretical studies indicated that high lithium salt concentration enhances the lithium ion transference number in the electrolytes.^[33,34,51] It is in accord with the Li^+ solvation ionic radius analysis by DFT calculation. The theoretical Raman spectrum of EC solvation Li^+ complexes with different solvent numbers is calculated (see

Fig. 2(b)). The C–H stretching vibration peaks are assigned to $3053.85\text{--}3173.16\text{ cm}^{-1}$, and with the decrease of the Li^+ concentration, it is slightly shifted to lower frequency. The C–H bond rotation vibration is assigned to the peaks at 1510 cm^{-1} and 1245.55 cm^{-1} . The vibration of EC ring enlargement is assigned to the peak of $888.85\text{--}916.78\text{ cm}^{-1}$, which shifts to low frequency when the EC molecule increases in $n\text{EC-Li}^+$ compounds. The different vibration signals are exhibited in the IR and Raman spectra respectively. The theoretical Raman spectrum of PC solvation Li^+ complexes is also calculated (see Fig. 2(c)). The peaks in $3033.66\text{--}3162.04\text{ cm}^{-1}$ are

C–H stretching vibration, and the C–H rotation vibration is assigned to the peaks at about 1500 cm^{-1} . The vibration peak at 858 cm^{-1} is the enlargement of PC ring. The theoretical Raman spectrum of DMC solvation Li^+ compounds is also calculated (see Fig. 2(d)). The peaks in $3051.73\text{--}3186.86\text{ cm}^{-1}$ are C–H stretching vibration. The C–H rotation vibration is assigned to the peak in $1494.96\text{--}1499.95\text{ cm}^{-1}$. The DMC total stretching vibration is assigned to the peak in $929.15\text{--}971.95\text{ cm}^{-1}$, which shifts to lower frequency when the DMC molecule increases in the $n\text{DMC-Li}^+$ compounds. The solvation state of electrolytes might be identified by the theoretical spectra.

Table 2. The O–Li bond and average length in $n\text{EC-Li}^+$, $n\text{PC-Li}^+$, and $n\text{DMC-Li}^+$, the unit is Å.

	O–Li	O–Li	O–Li	O–Li	O–Li	Average O–Li
EC-Li ⁺	1.739	–	–	–	–	1.739
2EC-Li ⁺	1.791	1.791	–	–	–	1.791
3EC-Li ⁺	1.857	1.857	1.856	–	–	1.857
4EC-Li ⁺	1.944	1.932	1.949	1.939	–	1.941
5EC-Li ⁺	1.930	1.945	1.986	1.933	5.094	2.577
PC-Li ⁺	1.735	–	–	–	–	1.735
2PC-Li ⁺	1.788	1.788	–	–	–	1.788
3PC-Li ⁺	1.855	1.857	1.855	–	–	1.856
4PC-Li ⁺	1.945	1.944	1.945	1.941	–	1.944
5PC-Li ⁺	1.931	1.985	1.945	1.931	4.803	2.519
DMC-Li ⁺	1.735	–	–	–	–	1.735
2DMC-Li ⁺	1.785	1.785	–	–	–	1.785
3DMC-Li ⁺	1.855	1.856	1.857	–	–	1.856
4DMC-Li ⁺	1.954	1.985	1.949	1.939	–	1.957
5DMC-Li ⁺	2.254	2.025	2.06	2.086	2.027	2.090

3.1.3. Infrared and Raman spectra for Li^+ solvation in DEC and EMC

The solvation of Li^+ by linear molecules of DEC and EMC is also studied. Figure 3(a) shows the ΔG plots for Li^+ solvation reactions with EMC and DEC, respectively. It is clearly exhibited that three DEC and DMC molecules can spontaneously combine one Li^+ forming 3sol-Li^+ solvation shell complexes at most respectively, and the solvation reaction energies are listed in Table 3. The further solvation reactions are non-spontaneous for $3\text{DEC-Li}^+ + \text{DEC} = 4\text{DEC-Li}^+$ and $3\text{EMC-Li}^+ + \text{EMC} = 4\text{EMC-Li}^+$ at 298.15 K . Figure 3(b) shows the solvation structures of DEC and EMC with Li^+ , it can be seen that Li^+ is surrounded by solvent molecules, and the inner core solvation shell can hold up four DEC or EMC molecules at most. The total solvation reaction energies for $5\text{DEC} + \text{Li}^+ = 5\text{DEC-Li}^+$ and $5\text{EMC} + \text{Li}^+ = 5\text{EMC-Li}^+$ are -115.316 kcal/mol and -116.072 kcal/mol , respectively.

Table 3. The ΔE , ΔH , and ΔG (in kcal/mol) for the solvation reactions between Li^+ and DEC, EMC respectively.

Reactions in Li^+ and solvents	ΔE	ΔH	ΔG
DEC + $\text{Li}^+ = \text{DEC-Li}^+$	-47.607	-48.047	-41.193
DEC + DEC-Li ⁺ = 2DEC-Li ⁺	-35.106	-34.604	-25.336
DEC + 2DEC-Li ⁺ = 3DEC-Li ⁺	-21.528	-20.898	-12.301
DEC + 3DEC-Li ⁺ = 4DEC-Li ⁺	-9.373	-10.087	5.854
DEC + 4DEC-Li ⁺ = 5DEC-Li ⁺	-1.702	0.404	5.331
EMC + $\text{Li}^+ = \text{EMC-Li}^+$	-46.042	-46.500	-39.482
EMC + EMC-Li ⁺ = 2EMC-Li ⁺	-34.414	-33.834	-25.512
EMC + 2EMC-Li ⁺ = 3EMC-Li ⁺	-19.564	-18.852	-10.513
EMC + 3EMC-Li ⁺ = 4EMC-Li ⁺	-8.469	-7.881	4.365
EMC + 4EMC-Li ⁺ = 5EMC-Li ⁺	-7.583	-6.963	1.492

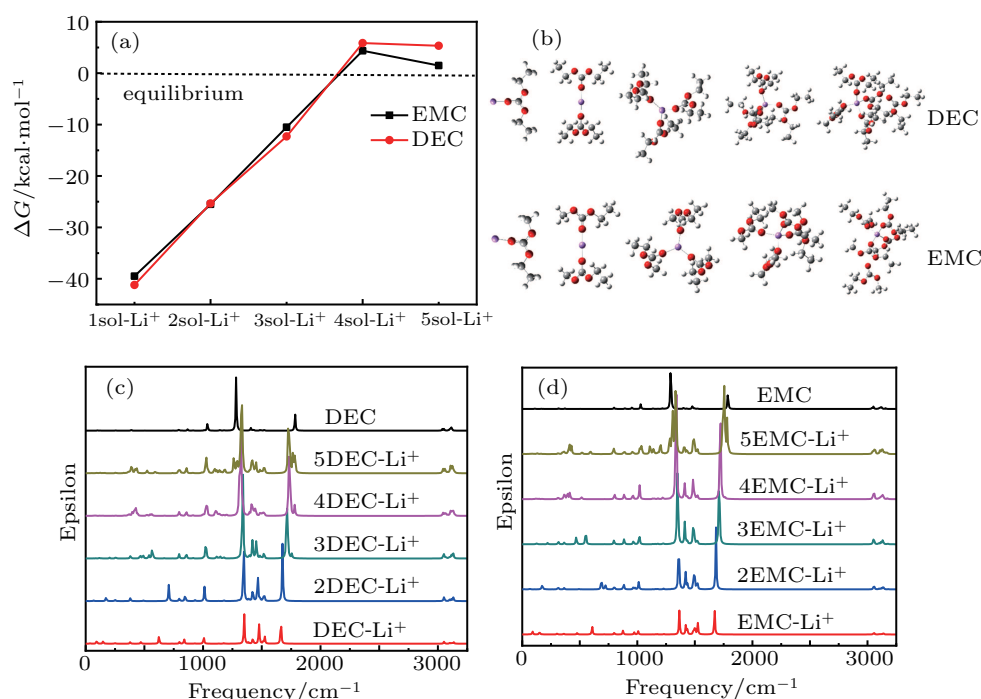


Fig. 3. (a) The ΔG plots for Li^+ solvation reactions with EMC and DEC respectively. (b) The solvation structure models of $n\text{DEC-Li}^+$ and $n\text{EMC-Li}^+$. White, dark gray, violet, and red spheres represent H, C, Li, and O ions/atoms, respectively. Theoretical infrared spectrum of (c) DEC and (d) EMC solvation Li^+ complexes with different Li^+ concentration.

Table 4 shows the O–Li bond and average length in $n\text{EMC-Li}^+$ and $n\text{DEC-Li}^+$ respectively. It is exhibited that the O–Li bond is shortened when the solvent number decreases in the Li^+ -solvation compounds, and the Li^+ solvation ionic radius is decreased when the lithium ion concentration increases in $n\text{EMC-Li}^+$ and $n\text{DEC-Li}^+$ compounds. The theoretical IR spectra of solvation compounds of DEC and Li^+ are calculated (see Fig. 3(c)). It is shown that the C=O stretching vibration is assigned in $1663.06\text{--}1783.74\text{ cm}^{-1}$, and it shifts to higher frequency when the DEC molecule increases. The stronger stretching vibration peak in $1281.52\text{--}1350.23\text{ cm}^{-1}$ is carbonate C–O, which shifts to lower frequency when the lithium ion concentration goes down. The stretching vibration peaks in $1005.79\text{--}1037.74\text{ cm}^{-1}$ are the C–C and C–O in $\text{CH}_3\text{CH}_2\text{O}$ group of $n\text{DEC-Li}^+$, it is slightly shifted to higher frequency when the concentration of Li^+ is reduced. Similar to DEC,

Table 4. The O–Li bond and average length in $n\text{EMC-Li}^+$ and $n\text{DEC-Li}^+$, the unit is Å.

	O–Li	O–Li	O–Li	O–Li	O–Li	Average O–Li
EMC-Li^+	1.731	–	–	–	–	1.731
2EMC-Li^+	1.783	1.783	–	–	–	1.783
3EMC-Li^+	1.853	1.854	1.856	–	–	1.855
4EMC-Li^+	1.978	1.959	1.942	1.945	–	1.956
5EMC-Li^+	1.968	1.932	1.922	1.977	4.594	2.479
DEC-Li^+	1.727	–	–	–	–	1.727
2DEC-Li^+	1.780	1.780	–	–	–	1.780
3DEC-Li^+	1.851	1.876	1.852	–	–	1.86
4DEC-Li^+	1.938	1.965	1.940	1.954	–	1.949
5DEC-Li^+	1.937	1.949	1.942	1.944	4.700	2.494

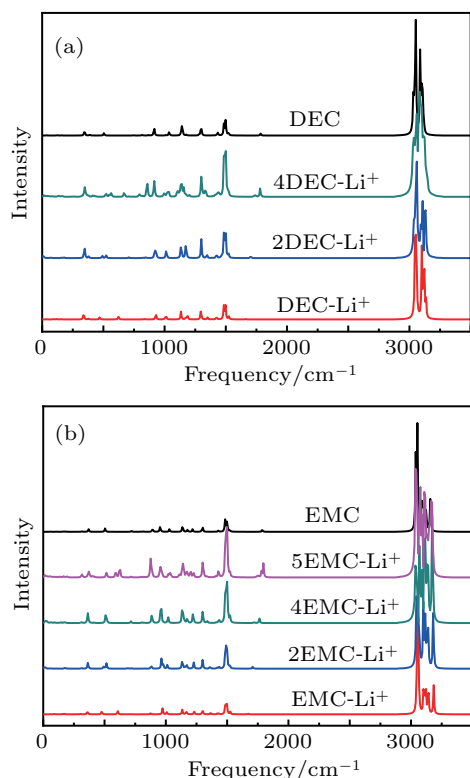


Fig. 4. (a) DEC and (b) EMC solvation- Li^+ compounds theoretical Raman spectrum analysis with different Li^+ concentration.

the peaks in $1671.37\text{--}1787.41\text{ cm}^{-1}$, $1290.57\text{--}1365.62\text{ cm}^{-1}$, and $1007.49\text{--}1029.72\text{ cm}^{-1}$ represent C=O, carbonate C–O, as well as O–C and C–C of $\text{CH}_3\text{CH}_2\text{O}$ stretching vibration in $n\text{EMC-Li}^+$, respectively, as shown in Fig. 3(d).

Theoretical Raman spectra of DEC and EMC solvation lithium ion complexes are also calculated. As shown in Fig. 4, the C–H stretching vibrations are assigned to the peaks in $3037.84\text{--}3134.9\text{ cm}^{-1}$ and $3038.14\text{--}3184.91\text{ cm}^{-1}$ for $n\text{DEC-Li}^+$ and $n\text{EMC-Li}^+$, respectively. In addition, the C–H rotation vibrations are assigned to the peaks in $1496.49\text{--}1498.74\text{ cm}^{-1}$ and $1496.61\text{--}1499.35\text{ cm}^{-1}$ for $n\text{DEC-Li}^+$ and $n\text{EMC-Li}^+$, respectively. The total stretching of DEC is assigned to the vibration peak in $1134.32\text{--}1143.58\text{ cm}^{-1}$. It is clearly seen that the peak signals in IR and Raman spectra are evidently different. The Raman spectra are agile to C–H vibration for the compounds of carbonate esters solvation with lithium ion, and the IR spectra are agile to C–O and C=O. It is important to study the solvation structure and frequency shift by the Raman and IR spectra combination analysis.

3.2. Analysis of ether-based solvation Li^+

3.2.1. Solvation and infrared spectrum for DOL, DME, and THF

Except for carbonate ester solvents, DOL, DME, and THF of ether based solvents are also calculated, there are commonly used in Li–S battery. Figure 5(a) exhibits the ΔG plots for Li^+ solvation reactions with DOL, DME, and THF, respectively, it is seen that cyclic DOL and THF can spontaneously combine Li^+ forming 4DOL-Li^+ and 4THF-Li^+ , and Li^+ is combined by three linear DME molecules to form 3DME-Li^+ compounds at most by stepwise solvation reactions. The solvation reaction energy is also shown in Table 5. It is non-spontaneous for the solvation reactions of $4\text{DOL-Li}^+ + \text{DOL} = 5\text{DOL-Li}^+$, $4\text{THF-Li}^+ + \text{THF} = 5\text{THF-Li}^+$, and $3\text{DME-Li}^+ + \text{DME} = 4\text{DME-Li}^+$ at 298.15 K . The total solvation reaction energies for $5\text{DOL} + \text{Li}^+ = 5\text{DOL-Li}^+$, $5\text{DME} + \text{Li}^+ = 5\text{DME-Li}^+$, and $5\text{THF} + \text{Li}^+ = 5\text{THF-Li}^+$ are -98.895 kcal/mol , -90.3449 kcal/mol , and -111.102 kcal/mol , respectively. It is concluded that the total solvation reaction energies for $5\text{sol} + \text{Li}^+ = 5\text{sol-Li}^+$ are -130.286 kcal/mol (5EC-Li^+), -132.2 kcal/mol (5PC-Li^+), -110.212 kcal/mol (5DMC-Li^+), -115.316 kcal/mol (5DEC-Li^+), -116.072 kcal/mol (5EMC-Li^+), -98.895 kcal/mol (5DOL-Li^+), -90.3449 kcal/mol (5DME-Li^+), -111.102 kcal/mol (5THF-Li^+), respectively. It is indicated that Li^+ solvation priority orders are $\text{PC} > \text{EC} > \text{EMC} > \text{DEC} > \text{THF} > \text{DMC} > \text{DOL} > \text{DME}$ to form 5sol-Li^+ .

The theoretical IR spectrum of $n\text{DOL-Li}^+$ solvation compounds is analyzed (see Fig. 5(b)). The C–H stretching vibration is assigned to the peaks in $2947.55\text{--}3164.42\text{ cm}^{-1}$,

and it is shifted to lower frequency when the Li^+ concentration is reduced. The two vibration peaks at 1111 cm^{-1} and 1177 cm^{-1} represent CH_2 group rotation for $n\text{DOL-Li}^+$, and it has no evident frequency shift when the DOL molecule number changes. The kinds of C–O stretching are assigned to the vibration peaks in $804.3\text{--}1048.72\text{ cm}^{-1}$, which shift to lower frequency evidently when the Li^+ concentration increases. In addition, the vibration peak around 500 cm^{-1} is Li–O stretching. Figure 5(c) shows the IR spectra of the solvation structure of DME with Li^+ . It is shown that the C–H stretching vibration is assigned to the peaks in $2734.3\text{--}3153.01\text{ cm}^{-1}$, and it shifts to lower frequency when the Li^+ concentration goes up. The shift rule is different from that of $n\text{DOL-Li}^+$. The different C–O stretching vibrations are assigned to the peaks at 924.9 cm^{-1} , 1039.4 cm^{-1} , 1093.3 cm^{-1} , and 1161.4 cm^{-1} , and it is shifted a little with the change of solvent molecule numbers. Figure 5(d) exhibits the spectra of THF with Li^+ solvation structures. It can be seen that C–H stretching is assigned to the vibration peaks in $2991.89\text{--}3128.91\text{ cm}^{-1}$, the frequency is shifted to higher direction with the increase of the

Li^+ concentration. The C–O stretching vibration is assigned to the two main peaks in $864.1\text{--}1096.4\text{ cm}^{-1}$, the frequency is evidently shifted to lower direction when the Li^+ concentration increases. Similar to DME, the vibration peak at about 500 cm^{-1} is the Li–O stretching.

Table 5. The ΔE , ΔH , and ΔG (in kcal/mol) for the solvation reactions between Li^+ and DOL, DME, and THF, respectively.

Reactions in Li^+ and solvents	ΔE	ΔH	ΔG
$\text{DOL} + \text{Li}^+ = \text{DOL-Li}^+$	-37.262	-37.910	-30.100
$\text{DOL} + \text{DOL-Li}^+ = 2\text{DOL-Li}^+$	-29.624	-29.236	-20.422
$\text{DOL} + 2\text{DOL-Li}^+ = 3\text{DOL-Li}^+$	-19.355	-19.561	-6.761
$\text{DOL} + 3\text{DOL-Li}^+ = 4\text{DOL-Li}^+$	-12.254	-11.337	-1.786
$\text{DOL} + 4\text{DOL-Li}^+ = 5\text{DOL-Li}^+$	-0.400	0.2586	11.108
$\text{DME} + \text{Li}^+ = \text{DME-Li}^+$	-38.902	-39.400	-32.274
$\text{DME} + \text{DME-Li}^+ = 2\text{DME-Li}^+$	-29.225	-28.617	-20.427
$\text{DME} + 2\text{DME-Li}^+ = 3\text{DME-Li}^+$	-17.308	-16.847	-6.388
$\text{DME} + 3\text{DME-Li}^+ = 4\text{DME-Li}^+$	-4.868	-4.709	9.380
$\text{DME} + 4\text{DME-Li}^+ = 5\text{DME-Li}^+$	-0.0419	1.364	4.568
$\text{THF} + \text{Li}^+ = \text{THF-Li}^+$	-43.359	-43.987	-36.229
$\text{THF} + \text{THF-Li}^+ = 2\text{THF-Li}^+$	-33.830	-33.453	-24.196
$\text{THF} + 2\text{THF-Li}^+ = 3\text{THF-Li}^+$	-21.442	-21.075	-10.366
$\text{THF} + 3\text{THF-Li}^+ = 4\text{THF-Li}^+$	-12.871	-12.318	-2.310
$\text{THF} + 4\text{THF-Li}^+ = 5\text{THF-Li}^+$	0.400	1.057	13.034

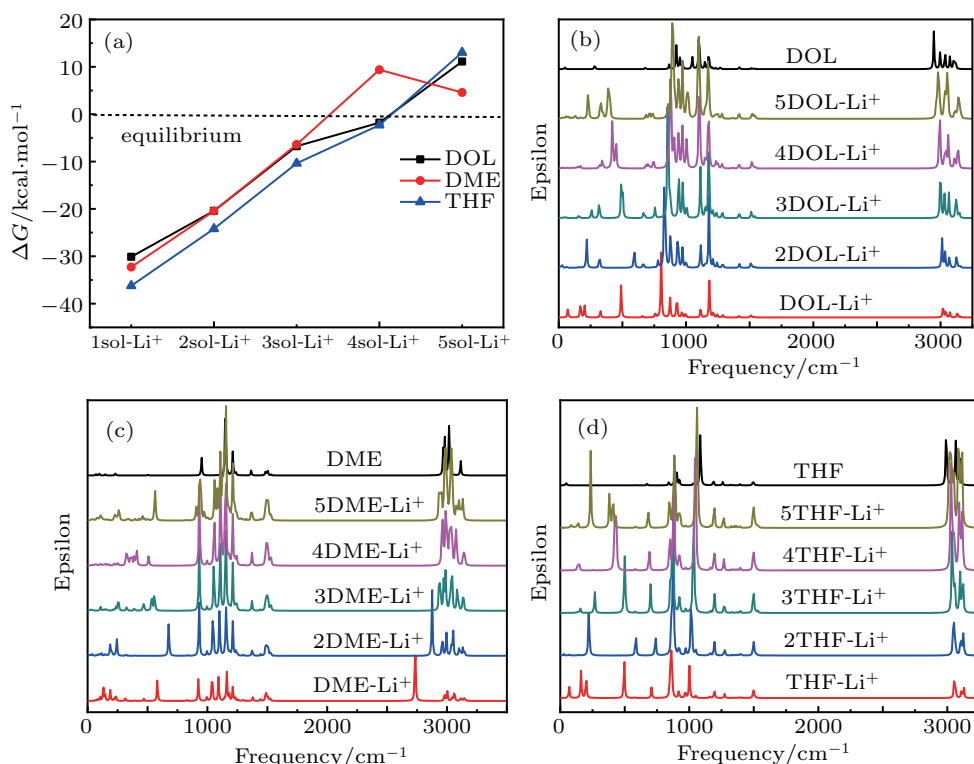


Fig. 5. (a) The ΔG plots for Li^+ solvation reaction with DOL, DME, and THF, respectively. Theoretical infrared spectrum of (b) DOL, (c) DME, and (d) THF solvation Li^+ complexes with different solvent numbers.

3.2.2. Theoretical Raman spectrum for Li^+ solvation in DOL, DME, and THF

The solvation structures of ether based $n\text{DOL-Li}^+$, $n\text{DME-Li}^+$, and $n\text{THF-Li}^+$ are shown in Fig. 6(a). It is clearly exhibited that Li^+ is surrounded by five solvent molecules forming inner solvation sheaths for cyclic DOL and THF sol-

vent. For linear DME, Li^+ is surrounded by four solvent molecules forming the inner solvation sheath at most. Table 6 shows the O–Li bonds and the average length in $n\text{DOL-Li}^+$, $n\text{DME-Li}^+$, and $n\text{THF-Li}^+$, respectively. The average O–Li bond lengths in DOL-Li^+ , 2DOL-Li^+ , 3DOL-Li^+ , 4DOL-Li^+ , and 5DOL-Li^+ are 1.806 \AA , 1.846 \AA , 1.899 \AA , 1.806 \AA , 1.846 \AA , 1.899 \AA , 1.806 \AA , 1.846 \AA , 1.899 \AA , 1.806 \AA , and 1.846 \AA , respectively.

1.972 Å, and 2.149 Å, respectively. The average O–Li bond lengths in DME-Li⁺, 2DME-Li⁺, 3DME-Li⁺, 4DME-Li⁺, and 5DME-Li⁺ are 1.811 Å, 1.849 Å, 1.913 Å, 2.039 Å, and 2.946 Å, respectively. The average O–Li bond lengths in THF-Li⁺, 2THF-Li⁺, 3THF-Li⁺, 4THF-Li⁺, and 5THF-Li⁺ are 1.793 Å, 1.837 Å, 1.894 Å, 1.970 Å, and 2.130 Å, respectively. It is exhibited that the O–Li bond is shortened when the solvent number decreases in the Li solvation compounds of *n*DOL-Li⁺, *n*DME-Li⁺, and *n*THF-Li⁺, and the Li⁺ solvation ionic radius is decreased when the lithium ion concentration increases. The results are in agreement with Li⁺ solvation in the carbonate ester solvents. Figure 6(b) shows the theoretical Raman spectrum of DOL solvation Li⁺ complexes with different solvent numbers. The C–H stretching vibration is assigned to the stronger peaks in 2947.55–3156.06 cm⁻¹, the frequency is evidently shifted to higher direction with the increase of the Li⁺ concentration. The vibration peak in 1508 cm⁻¹ is ascribed to C–H rotation. The C–H stretching of *n*DME-Li⁺ is assigned to the vibration peaks in 2734.3–3153.01 cm⁻¹, as shown in Fig. 6(c), the frequency shift is different from that of *n*DOL-Li⁺. The C–H rotation vibration is assigned to the peaks around 1503 cm⁻¹. The total stretching of *n*DME-Li⁺ is assigned to the vibration peak in 951.37–996.12 cm⁻¹, it is slightly shifted to higher frequency when the solvent molecule is reduced. The Raman spectra of THF solvation with Li⁺ are shown in Fig. 6(d). It is exhibited that the C–H stretch-

ing vibration is assigned to the stronger peaks in 2996.51–3128.91 cm⁻¹, and the peaks frequency is evidently shifted to higher direction with the increase of the Li⁺ concentration. In addition, the two vibration peaks at 895 cm⁻¹ and 929.1 cm⁻¹ are ascribed to the total stretching of THF and C–C stretching, respectively.

On the other hand, the temperature change also affects the solvation reaction energies (ΔE), enthalpies (ΔH), and free energies (ΔG), further study in Li⁺ solvation needs to be done at different temperatures to deeply investigate the Li⁺ solvation mechanism for lithium ion battery.

Table 6. The O–Li bond and average length in *n*DOL-Li⁺, *n*DME-Li⁺, and *n*THF-Li⁺, the unit is Å.

	O–Li	O–Li	O–Li	O–Li	O–Li	Average O–Li
DOL-Li ⁺	1.806	–	–	–	–	1.806
2DOL-Li ⁺	1.846	1.846	–	–	–	1.846
3DOL-Li ⁺	1.900	1.902	1.896	–	–	1.899
4DOL-Li ⁺	1.952	1.985	1.969	1.981	–	1.972
5DOL-Li ⁺	2.242	2.060	2.356	2.044	2.044	2.149
DME-Li ⁺	1.811	–	–	–	–	1.811
2DME-Li ⁺	1.849	1.849	–	–	–	1.849
3DME-Li ⁺	1.909	1.913	1.917	–	–	1.913
4DME-Li ⁺	2.052	2.020	2.035	2.047	–	2.039
5DME-Li ⁺	1.906	1.905	1.899	4.514	4.505	2.946
THF-Li ⁺	1.793	–	–	–	–	1.793
2THF-Li ⁺	1.837	1.837	–	–	–	1.837
3THF-Li ⁺	1.891	1.895	1.897	–	–	1.894
4THF-Li ⁺	1.965	1.973	1.975	1.966	–	1.970
5THF-Li ⁺	2.241	2.062	2.063	2.267	2.016	2.130

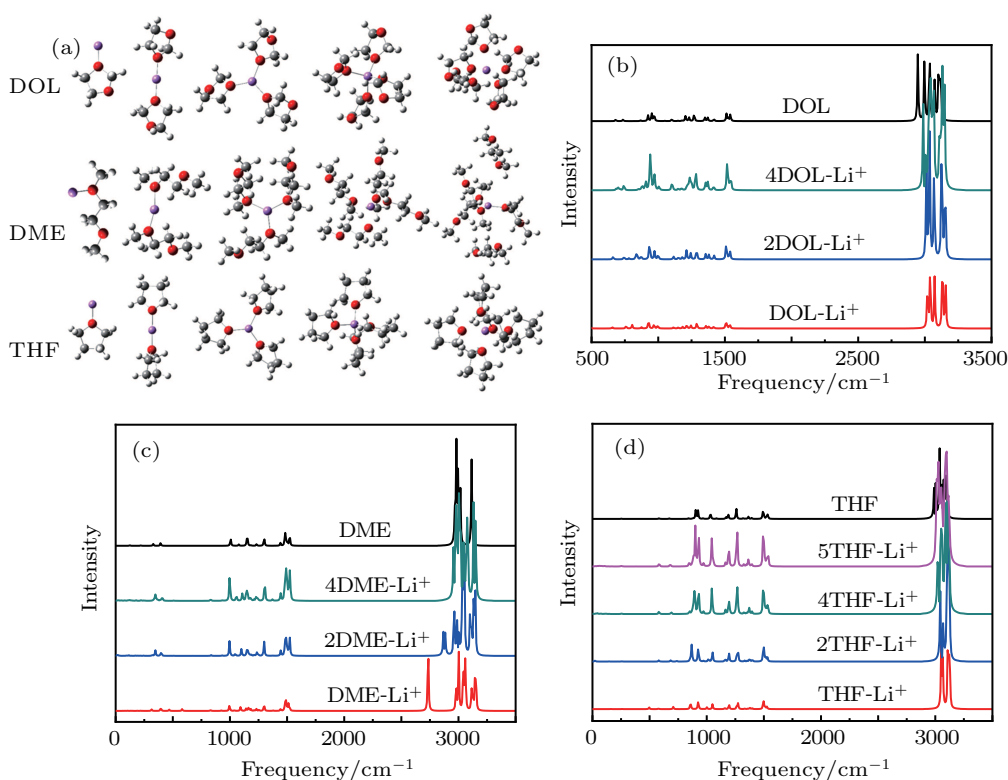


Fig. 6. (a) The solvation structure models of *n*DOL-Li⁺, *n*DME-Li⁺, and *n*THF-Li⁺. White, dark gray, violet, and red spheres represent H, C, Li, and O ions/atoms, respectively. Theoretical Raman spectra of (b) DOL, (c) DME, and (d) THF solvation Li⁺ complexes with different Li⁺ concentration.

4. Conclusion

The Li⁺ solvation in common carbonate ester and ether based solvents and their theoretical IR and Raman spectra are calculated by DFT method. It is demonstrated that the stepwise solvation reactions of sol + 3sol-Li⁺ = 4sol-Li⁺ are spontaneous to form innermost solvation shell complexes for the cyclic solvents of EC, PC, DOL, and THF at 298.15 K. But for the linear molecules of DEC, DMC, EMC, and DME, the maximum spontaneous solvation reactions are sol + 2sol-Li⁺ = 3sol-Li⁺. The solvation reaction energy results demonstrate that the Li⁺ solvation priority orders are PC > EC > EMC > DEC > THF > DMC > DOL > DME to form 5sol-Li⁺. It is demonstrated that the Li⁺-solvation ionic radius is decreased when the lithium ion concentration increases. The decrease of the Li⁺ solvation ionic radius may enhance its mobility. It is also demonstrated that the C=O bond vibration peaks shift to lower frequency and the C-O peaks shift to higher frequency in carbonate ester solvents when the Li⁺ concentration increases in the solvation complexes. It is indicated that all Li-O stretching vibration peaks shift to higher frequency when the concentration of Li⁺ increases until 2sol-Li⁺. All C-H stretching vibration peaks shift to higher frequency with the increase of the Li⁺ concentration except for *n*DME-Li⁺ solvation complex. The calculation results also demonstrate that the Raman spectrum is more agile to characterize C-H vibration and IR is agile to O=C, O-C, and Li-O vibrations. It is important to deeply understand the solvation mechanism by combination analysis of IR and Raman spectra, which provides a guidance to design and characterize different Li salt concentration electrolytes.

References

- Zhang Y, Yu C, Yang M, Zhang L R, He Y C, Zhang J Y and Yan H 2017 *Chin. Phys. Lett.* **34** 038101
- Wang J M, Chen K, Xie W G, Shi T T, Liu P Y, Zheng Y F and Zhu R 2019 *Acta Phys. Sin.* **68** 158806 (in Chinese)
- Yang Z G, Zhang J L, Kintner-Meyer M C W, Lu X C, Choi D W, Lemmon J P and Liu J 2011 *Chem. Rev.* **111** 3577
- Etacheri V, Marom R, Elazari R, Salitra G and Energ. D 2011 *Energ. Environ. Sci.* **4** 3243
- Armand M and Tarascon J M 2008 *Nature* **451** 652
- Alias N and Mohamad A A 2015 *J. Power Sources* **274** 237
- Freire M, Kosova N V, Jordy C, Chateigner D, Lebedev O I, Maignan A and Pralong V 2016 *Nat. Mater.* **15** 173
- Goodenough J B 2018 *Nat. Electron.* **1** 204
- Wu B, Bi J, Liu Q, Mu D, Wang L, Fu J and Wu F 2019 *Electrochim. Acta* **298** 609
- Urbonaitė S, Poux T and Novák P 2015 *Adv. Energ. Mater.* **5** 1500118
- Wang Z, Dong Y, Li H, Zhao Z, Wu H B, Hao C and Lou X W D 2014 *Nat. Commun.* **5** 5002
- Chung S H, Chang C H and Manthiram A 2016 *Energ. Environ. Sci.* **9** 3188
- Yin Y X, Xin S, Guo Y G and Wan L J 2013 *Angew. Chem. Int. Edit.* **52** 13186
- Lu Y, Gu S, Hong X, Rui K, Huang X, Jin J and Wen Z 2018 *Energ. Storage Mater.* **11** 16
- Xu K 2004 *Chem. Rev.* **104** 4303
- Xu K 2014 *Chem. Rev.* **114** 11503
- Liu Q, Zhao Z, Wu F, Mu D, Wang L and Wu B 2019 *Solid State Ionics* **337** 107
- An S J, Li J, Daniel C, Mohanty D, Nagpure S and Wood III D L 2016 *Carbon* **105** 52
- Edström K, Gustafsson T and Thomas J O 2004 *Electrochim. Acta* **50** 397
- Liu Q, Mu D, Wu B, Xu H, Wang L, Gai L and Wu F 2017 *J. Electrochem. Soc.* **164** A3144–A3153
- Patel M U, Demir-Cakan R, Morcrette M, Tarascon J M, Gaberscek M and Dominko R 2013 *ChemSusChem.* **6** 1177
- Zhang S S 2012 *Electrochim. Acta* **70** 344
- Liu Q, Mu D, Wu B, Wang L, Gai L and Wu F 2017 *RSC Adv.* **7** 33373
- See K A, Leskes M, Griffin J M, Britto S, Matthews P D, Emly A and Seshadri R 2014 *J. Am. Chem. Soc.* **136** 16368
- Matsuda Y, Fukushima T, Hashimoto H and Arakawa R 2002 *J. Electrochem. Soc.* **149** A1045–A1048
- Borodin O and Smith G D 2006 *J. Phys. Chem. B* **110** 4971
- Yamada Y, Koyama Y, Abe T and Ogumi Z 2009 *J. Phys. Chem. C* **113** 8948
- Bhatt M D, Cho M and Cho K 2010 *Appl. Sur. Sci.* **257** 1463
- Yang L, Xiao A and Lucht B L 2010 *J. Mol. Liq.* **154** 131
- Bogle X, Vazquez R, Greenbaum S, Cresce A V W and Xu K 2013 *J. Phys. Chem. Lett.* **4** 1664
- Okoshi M, Yamada Y, Yamada A and Nakai H 2013 *J. Electrochem. Soc.* **160** A2160–A2165
- Bhatt M D and O'Dwyer C 2014 *Curr. Appl. Phys.* **14** 349
- Suo L, Hu Y S, Li H, Armand M and Chen L 2013 *Nat. Commun.* **4** 1481
- Wu B, Liu Q, Mu D, Ren Y, Li Y, Wang L and Wu F 2014 *J. Phys. Chem. C* **118** 28369
- Doi T, Masuhara R, Hashinokuchi M, Shimizu Y and Inaba M 2016 *Electrochim. Acta* **209** 219
- Wang J, Yamada Y, Sodeyama K, Chiang C H, Tateyama Y and Yamada A 2016 *Nat. Commun.* **7** 12032
- Ong M T, Verners O, Draeger E W, Van Duin A C, Lordi V and Pask J E 2015 *J. Phys. Chem. B* **119** 1535
- Seo D M, Reininger S, Kutcher M, Redmond K, Euler W B and Lucht B L 2015 *J. Phys. Chem. C* **119** 14038
- Logan E R, Tonita E M, Gering K L, Li J, Ma X, Beaulieu L Y and Dahn J R 2018 *J. Electrochem. Soc.* **165** A21
- Liu Q, Cresce A, Schroeder M, Xu K, Mu D, Wu B and Wu F 2019 *Energ. Storage Mater.* **17** 366
- Shi S, Gao J, Liu Y, Zhao Y, Wu Q, Ju W, Ouyang C and Xiao R 2016 *Chin. Phys. B* **25** 018212
- Skarmoutsos I, Ponnuchamy V, Vetere V and Mossa S 2015 *J. Phys. Chem. C* **119** 4502
- Bhatt M D, Cho M and Cho K 2012 *J. Solid State Electr.* **16** 435
- Bhatt M D, Cho M and Cho K 2012 *Model. Simul. Mater. Sci.* **20** 065004
- Li Z, Smith G D and Bedrov D 2012 *J. Phys. Chem. B* **116** 12801
- Cui W, Lansac Y, Lee H, Hong S T and Jang Y H 2016 *Phys. Chem. Chem. Phys.* **18** 23607
- Borodin O, Olguin M, Ganesh P, Kent P R, Allen J L and Henderson W A 2016 *Phys. Chem. Chem. Phys.* **18** 164
- Chaban V 2015 *Chem. Phys. Lett.* **631–632** 1
- Hou B, Gan Z, et al. 2019 *Acta Phys. Sin.* **68** 128801 (in Chinese)
- Frisch M J, Trucks G W, Schlegel H B, et al. 2010 *Gaussian 09* Gaussian, Inc., Wallingford, CT
- Liu Q, Xu H, Wu F, Mu D, Shi L, Wang L, Bi J and Wu B 2019 *ACS Appl. Energy Mater.* **2** 8878